Supplementary Data

Biomechanical defects and rescue of cardiomyocytes expressing pathologic nuclear lamins

Erik Laurini[1§], Valentina Martinelli[2§], Thomas Lanzicher[1§], Luca Puzzi[1], Daniele Borin[1], Suet Nee Chen[3], Carlin S. Long[3], Patrice Lee[4], Luisa Mestroni[3], Matthew R.G. Taylor[3], Orfeo Sbaizero[1], Sabrina Pricl[1]

[§]*share authorship*

Materials & Methods:

Isolation and culture of ventricular cardiomyocytes from neonatal rat (NRVMS)

Animal care and treatment were in accordance with the Italian and EU laws (*D. Lgs n° 2014/26, 2010/63/EU*). Methods for NRVMs isolation and culture have previously been described[1, 2]. All animal experiments have been done using all possible methods to alleviate or minimize potential pain, suffering or distress, and enhance animal welfare. Animals have been provided with housing in an enriched environment, with at least some freedom of movement, food, water and daily care and cleaning. The well-being and state of health of experimental animals will be observed by competent persons, dedicated to the management of the Animal House, capable to prevent pain or avoidable suffering, distress or lasting harm. Experiments have been performed solely by competent authorized persons. Primary cultures of neonatal rat ventricular cardiomyocytes (NRVMs) were isolated and cultured from 1-3 days old Wistar rat pups following decapitation by enzymatic digestion as previously described with minor modifications[3-6]. Briefly, ventricles were separated from the atria using scissors and then dissociated in CBFHH (calcium and bicarbonate-free Hanks with Hepes) buffer containing 0.5 mg/ml of Collagenase type 2 (Worthington, Biochemical Corporation), and 1 mg/ml of Pancreatine (SIGMA). Cardiomyocytes were enriched (>90% purity) over non-myocytes by a pre-plating step on 100-mm dishes in Dulbecco's modified Eagle Medium (DMEM) 4.5g of glucose, supplemented with 10% FBS and 2 mg/ml vitamin B12 (SIGMA). Myocytes that were either in solution or lightly attached were then

separated from the adherent stromal cells by gentle mechanical disaggregation and subsequently plated at a density of 2x105 cells/ml in primary petri dishes (FALCON) or in multichamber slides coated with 0.02% gelatin plus Fibronectin 1mg/ml (SIGMA) and cultured as previously described[3, 4]. After 18 h, the culture medium was changed and cells were subjected to infection with the relevant adenoviral-LMNA constructs.

Isolation Adenoviral constructs and infection

Methods for adenoviral infection have been previously reported[1, 2]. In brief, shuttle constructs were generated in Dual CCM plasmid DNA containing GFP gene and human LMNA cDNA. Constructs were bicistronic with the two inserts (LMNA and GFP) driven by two different CMV promoters to identify cells expressing LMNA protein using GFP as a marker of cellular infection. Constructs contained either human wild-type or the human mutant LMNA genes. The construct carrying only GFP gene was used as a control to assess infection efficiency. NRVMs were infected by adenoviruses at 25 multiplicity of infection (MOI) in serum free medium; 6 hours post-infection, complete medium was replaced to cardiomyocytes and the cells were incubated at 37°C and 5% CO_2. Previous control experiments have shown that GFP transfection and expression did not affect endpoints of interest in NRVM in our experimental conditions[1].

Western Blotting

For protein analysis, transduced cells were lysed in Ripa Buffer 1X and protein concentration was determined by Bradford method (Bio-Rad Laboratories). Equal amount of protein was then resolved on 10% SDS-PAGE gel and blotted in 10% nonfat milk in PBS-T. Membranes were incubated with primary antibodies in PBS/ goat serum (Gibco) overnight at 4C. Secondary antibodies were incubated with the membranes for 45 min at room temperature. Protein detection was performed by enhanced chemiluminescence (GE Healthcare).
The primary antibodies used were as follows: rabbit polyclonal LMNA/LAMIN A+C (aa59-572) LS-C186225 1:2000, (LSBio, LifeSpan BioSciences, Inc.), rabbit Anti-Lamin A (C-terminal) L 1293, 1:2000 (SIGMA), rabbit GAPDH FL-335, 1:5000 (Santa Cruz Biothecnology). Secondary antibody used was anti-rabbit HRP-conjugated, 1:2000 (DAKO).

Immunofluorescence

NRVMs were fixed in PBS containing 4% PFA for 20 min at room temperature, aldehydes were quenched with 0.1 M glycine in PBS for 20. Cells were permeabilized at room temperature, with 1%Triton X-100 for 30 min, blocked with 10% goat serum (GS) in PBS for 1 h and incubated with Alexa Fluor 594 Phalloidin (Life Technologies) at 1:500 dilution for 45 min in PBS, at room temperature. Each slide was then mounted in Vectashield with DAPI (Vector Labs) to counter-staining the nuclei. Representative immunofluorescence images were acquired by using NIKON A1 plus Confocal microscope (NIKON Eclipse Ti), equipped with Plan-Apochromat 60X/1.40 oil objective and with ZEISS LSM 800 with Ayriscan. In order to obtain complete 3D reconstructions of NRVM, 25 images were acquired for a total extension of 8.5 μm on the z-axes. Expression of human wild-type and mutant LMNA proteins were verified by western blot to confirm exogenous human LMNA in NRVMs together with the endogenous rat level expression.

ARRY-371797administration

Following 24 hours of cardiomyocytes isolation, ARRY-371797 was administrated to the cell culture. Briefly, cells were washed in PBS and the complete neonatal cardiomyocytes medium removed. Cells were treated in triplicate with fresh complete medium supplemented with ARRY-371797 in a final concentration of 0.1 and 1 μM in DMSO diluted. The final concentration was determined based on a titration experiment, where higher concentrations, not achievable in vivo, were found to alter significantly the biomechanical properties in controls NRVM (data not shown). Cells were finally incubated at 37 for 3 hours, and then used for AFM experiments or fixed for immunofluorescence analysis.

Molecular modeling

Dimeric WT and mutant LAMA model building and optimization.

Nanomechanical simulations.

All steered molecular dynamics (SMD) simulations were carried out using NAMD (v. 2.10) and the CHARMM22 force field[7]. This force field has already been successfully validated in similar studies and, specifically, on closely related intermediate filaments[7-12]. To apply the force that induces molecular deformation, the alpha-carbon (Cα) atoms at one end of the dimeric protein structure are kept fixed in time and space, while the force is applied the corresponding Cα at the opposite end. In this respect, this *in silico*

experiment (SMD) plainly resembles the AFM experiment in which one end of the protein under examination is (covalently) linked onto a given surface while the other end is pulled by the AFM cantilever tip. According to the SMD method, the force *F* that pull atom can be described by Hook's law: $F = k(v \times t - x)$, where *k* is the spring constant, *v* is the pulling velocity, *t* is the simulation time step and *x* is the corresponding atom displacement. Following the conditions previously optimized for vimentin[9, 11-13] in this study we set the *k* value to 10 kcal/mol/Å while the pulling rate v was fixed to 1 m/s. During the SMD trajectory, both the force *F* and position *x* of the pulled atom(s) is monitored over time, ultimately yielding the force vs displacement curve. The subsequent analysis of the mechanical properties of the simulated system is easily performed by introducing the so-called engineering strain, defined as: $\varepsilon = \Delta L/L_0$, in which $\Delta L = x - x_0$ and x_0 is the initial length of the molecule undergoing the tensile loading simulation. By definition, the corresponding engineering stress is given by: $\sigma = F/A_0$, where *F* is the pulling force and A_0 is the molecular cross-sectional area. According to the present *LMNA* dimer model, the average radius of the molecular cross-section was set equal to 10.2 Å, therefore, the corresponding value of $A_0 = 327$ Å^2 (obtained assuming a circular cross section of the protein) was employed in the formulas above.

Finally, the Young's modulus *E* for each *LMNA* protein was extracted from the respective $\sigma = f(\varepsilon)$ curve by determining the slope of this curve in regime I, i.e., when the linear elastic regime was at play.

AFM – Single Cell Force Spectroscopy

An AFM Solver Pro-M (NT-MDT, Moscow, Russia) was used to acquire morphology as well as force-displacement curves. In AFM test, it is very important to bear in mind that cells can be in different states and thus show distinct properties that can be difficult to compare. Therefore (i) cells have been prepared following a strict protocol for each cell type. Moreover, AFM experiments were always performed on the same day they were collected for biochemical (expressions) analyses, (ii) multiple measurements from different cells have been collected to control for variability and 'average' data determined, and (iii) cells were monitored and their morphological details observed (an optical light microscope was used for cell selection throughout the tests). The AFM was equipped with a "liquid cell" setup with a standard cantilever holder cell for operating in liquid at controlled temperature. A probe modified with polystyrene microsphere (diameter of ~7 μm) coated with a layer of gold was used to precisely apply a compression force 'normal' to the nucleus. Polystyrene bead, is not

a truly rigid body however, the polystyrene Young modulus is about $3x10^9$ Pa much higher than that we measured for our nuclei (around $1x10^3$ Pa). For soft biological samples, it is suggested to use spherical probes since the force is applied to a broader cell area than would be the case if a sharp tip is used, resulting in a lower pressure and less cell damage. But this is not the only reason to prefer spherical indenters. Cells or tissues are very inhomogeneous, consisting of different components (nucleus, cytoskeletal components, etc.), therefore a spherical tip will return superior data for such inhomogeneous materials than a sharp tip. AFM probes were cleaned, prior to the indentation experiments, by embedding them successively in Tween (2% for 30 min), in order to remove contaminant molecules adsorbed on the probe surface. All studies were performed on living, intact cells in cell culture medium. Only well-spread and isolated cells were investigated. Those with a round shape and a dark edge were rejected. Furthermore, cardiomyocytes were selected based on the morphological aspect compared to the possible presence of fibroblasts and only if they were beating. The basic AFM technique for quantitative analysis of the cell elasticity is the force spectroscopy (called force-curve analysis). The relation between displacement and indentation of the cantilever in contact with the cell was obtained on extending and retracting curves, called force curves. Force curves were collected by monitoring cantilever deflection while moving the piezoscanner resulting in a plot of force versus sample position. Indentation depth is calculated comparing the curve detected on the glass substrate and the curve recorded on the cell. To calibrate the cantilever deflection signal, curves of force versus the piezo displacement were acquired on the hard substrate of the cells (glass). The AFM tip was moved toward the cell with speeds of 1 μm/s. The speed range was chosen to avoid cell movement (at low compression speed) or hydrodynamic force contribution (significant at high speed). The distal regions, away from the nucleus, were avoided since measurements performed around the nucleus are less affected by artifacts due to the substrate stiffness. All experiments were performed at the same velocity since these AFM tests are rate-dependent. We assessed the nuclear elasticity using at least 40 cells for each condition (CT, WT and three mutated conditions) and the same operators performed the experiments. These data were enough to detect statistically significant differences. The test duration was never longer than 45-50 min to ensure cells viability.

Modeling cells elasticity

The Young's modulus (elasticity) is often used to describe mechanical properties of cells. Since the earliest AFM studies of soft biological samples, the prevalent method of evaluating AFM indentation data to assess the elasticity has been the so-called "Hertz-Sneddon model" of contact between two elastic bodies.

The Hertz model assumes homogeneity, absolute cell elastic behavior and no interactions between sample and probe[14, 15]. But most biological materials are neither homogeneous nor absolutely elastic. In this case, the Hertz model is only valid for small indentations (up to 10% of the height of the cell). The Hertz model gives an estimation of the cell elasticity and it is clear that in any case it will be afflicted by an error since it requires the assumption that contact surfaces are uninterrupted and frictionless and their deformations are insignificant. Although, in the case of cells, these assumptions do not correspond completely to reality due to the heterogeneous cell structure, the Hertz model is still useful for achieving information about cell elasticity. However, it be should pointed out that elasticity values calculated using various models differ from each other[16, 17]. However, we believe that since all our tests have been performed with the same protocol, results can give a good estimate of the cells elasticity. Equation used is detailed in supplementary material.

In the present paper, we used the Hertz-Sneddon model for spherical tips[18].

$$F = \frac{4\,E\,\sqrt{R}}{3\,(1-\upsilon^2)}\,\delta^{3/2} \qquad (1)$$

Where F is the load force, E is the Young modulus, ν the Poisson ratio, δ is the probe penetration into the cell. The Poisson's ratio was assumed to be 0.5. Finally, cardiomyocytes that exhibited contractile activity (less than 15% of total cell number) were not included in the analysis due to the difficulty in establishing a reliable baseline.

Plasticity index

If the cell response is elastic, the AFM indentation and retraction curves should be identical, however, very often there is a considerable difference between these two curves. This *hysteresis* indicates that the response is not purely elastic. To quantify the relative amount of energy that was lost due to hysteresis during the AFM experiments, we used the plasticity index ζ[19], a parameter that characterizes the relative elastic-plastic behavior of the material when it is loaded. It is determined from the ratio between areas under loading (A_1) and unloading (A_2) which gives:

$$\zeta = 1 - (\frac{A_2}{A_1}) \qquad (2)$$

The plasticity index varies between $\zeta = 0$, when $A_1 = A_2$, thus loading and unloading are equal (fully *elastic* behavior), and $\zeta = 1$ when $A_2 = 0$ (fully *plastic*), while the intermediate values $0 < \zeta < 1$ indicate mixed viscoelastic properties.

Statistics

Experimental AFM data were analyzed using GraphPad Prism software. All data were first subjected to Shapiro normality test and then ordinary one-way ANOVA with Holm-Sidak's multiple comparisons test for normal distributions or the Kruskal-Wallis test with a Dunn's multiple comparisons test otherwise, both with a two-tailed *P*-value, were employed. Data in the text are reported as mean (normal distribution) or median (non-normal distribution) values ± standard error. Every experiment had plated cells obtained from more than 20 pups, for each preparation. For the outcome analysis of LMNA mutation carriers, we considered the combined events of death and heart transplant, and used the 2 tailed Fisher test (not adjusted for age) to compare the outcomes of death or cardiac transplant occurring before age 40 years for the *LMNA* D192G and N195K groups.

Supplement Figures

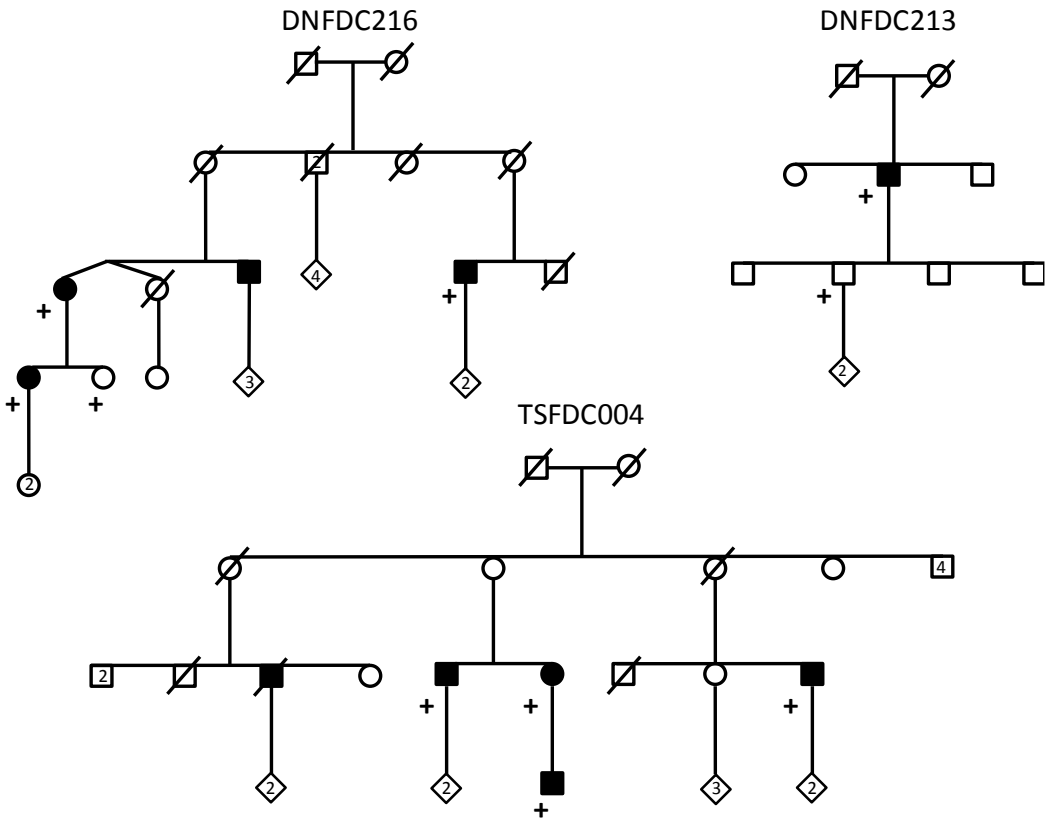

Figure 1S. Family pedigree are shown with males and females indicated by squares and circles, respectively. Individuals with dilated cardiomyopathy are indicated in black shading and individuals with confirm E161K *LMNA* mutation are indicated by the plus sign "+". Deceased individuals are indicated by the horizontal lines.

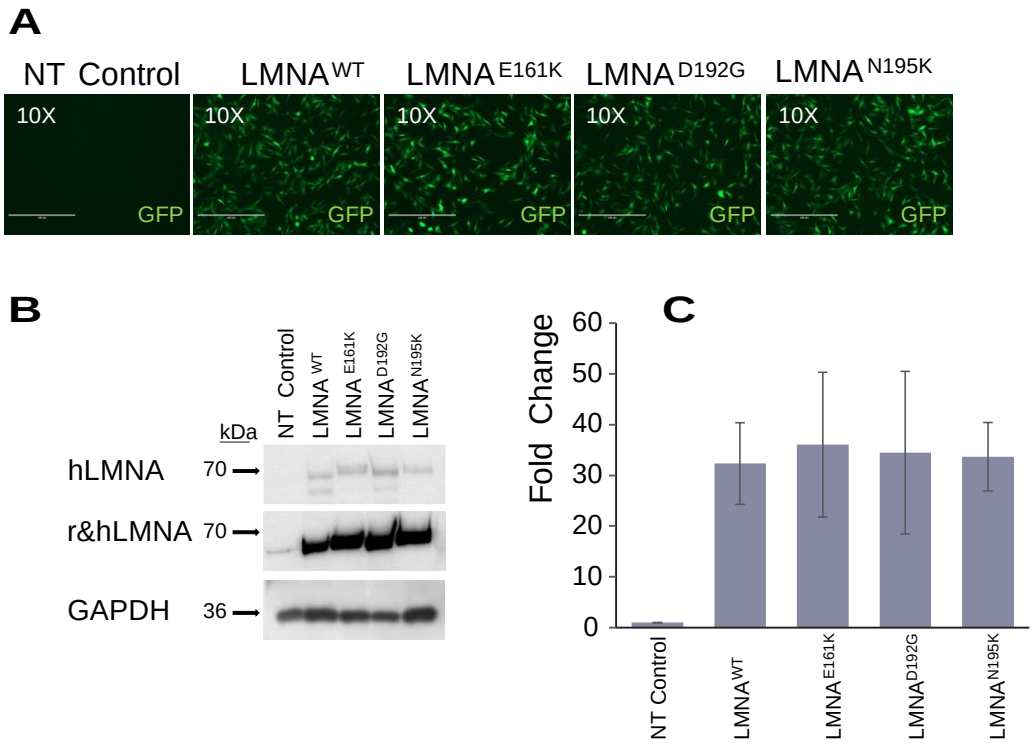

Figure 2S. LMNA expression in NRVM infected with AdV-*LMNA*^{WT}, AdV-*LMNA*^{Mutants} and non-treated uninfected (NT) control. (A) EGFP 48 hours post-infection with AdV-WT and mutant LMNA constructs (scale bar = 400 μm). (B) Expression of the transduced human LMNA protein detected by human specific anti-LMNA antibody (hLMNA) and expression of the total endogenous rat LMNA and transduced human LMNA protein detected by antibody able to detect both rat and human LMNA protein (r&hLMNA) by western blot 48 hours post-infection in purified NRVM. Representative blot demonstrates high human LMNA protein expression in infected NRVM compared to endogenous rat LMNA protein in NT NRVM. A housekeeping gene, GAPDH, is also shown. C) Bar graph showing fold change of expressed transduced human LMNA protein normalized to basal rat LMNA protein level (n=3).

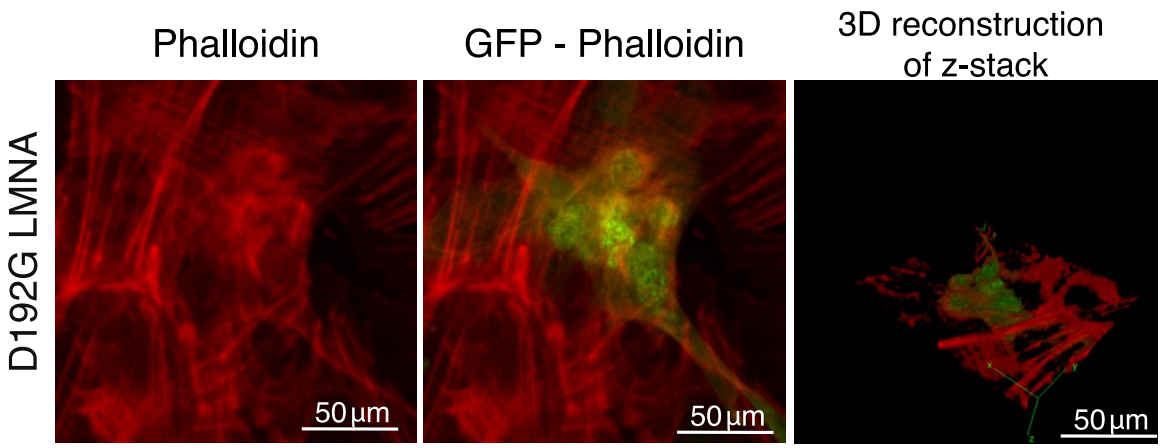

Fig. 3S. D192G LMNA mutant displays an extensive cytoskeletal alteration in NRVMs.

Representative images of fluorescently stained actin cytoskeleton of D192G LMNA mutant cells. Cells were stained with fluorescent phalloidin (which specifically stains F-actin, red). Extensive cytoskeletal network alteration was evident. The cytoskeleton of mutant appeared in a lower actin fiber density and distribution when compared with WT LMNA cells. The detailed structure of actin morphology was clearly visible in a 3D reconstruction of z-stack acquired in a range of 10um. Scale bar 50µm (n=4)

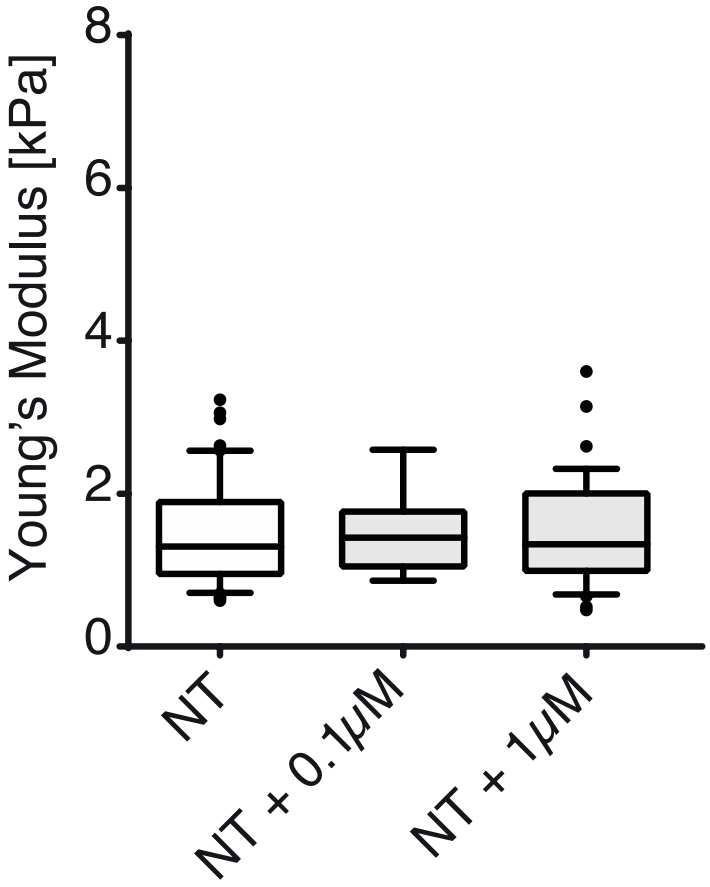

Figure 4S. Influence of the p38 MAPK inhibitor ARRY-371797 on control NT NRVM elasticity (independent experiments n=6, number of cells N= 51NT, after infection N>25)

References

1. Lanzicher T, Martinelli V, Puzzi L, Del Favero G, Codan B, Long CS, Mestroni L, Taylor MR, Sbaizero O. The Cardiomyopathy Lamin A/C D192G Mutation Disrupts Whole-Cell Biomechanics in Cardiomyocytes as Measured by Atomic Force Microscopy Loading-Unloading Curve Analysis. *Sci Rep* 2015;**5**:13388.
2. Lanzicher T, Martinelli V, Long CS, Del Favero G, Puzzi L, Borelli M, Mestroni L, Taylor MR, Sbaizero O. AFM single-cell force spectroscopy links altered nuclear and cytoskeletal mechanics to defective cell adhesion in cardiac myocytes with a nuclear lamin mutation. *Nucleus* 2015;**6**:394-407.
3. Martinelli V, Cellot G, Toma FM, Long CS, Caldwell JH, Zentilin L, Giacca M, Turco A, Prato M, Ballerini L, Mestroni L. Carbon nanotubes promote growth and spontaneous electrical activity in cultured cardiac myocytes. *Nano Lett* 2012;**12**:1831-1838.

4. Martinelli V, Cellot G, Fabbro A, Bosi S, Mestroni L, Ballerini L. Improving cardiac myocytes performance by carbon nanotubes platforms. *Front Physiol* 2013;**4**:239.
5. Long CS, Kariya K, Karns L, Simpson PC. Sympathetic modulation of the cardiac myocyte phenotype: studies with a cell-culture model of myocardial hypertrophy. *Basic Res Cardiol* 1992;**87 Suppl 2**:19-31.
6. Deng XF, Rokosh DG, Simpson PC. Autonomous and growth factor-induced hypertrophy in cultured neonatal mouse cardiac myocytes. Comparison with rat. *Circ Res* 2000;**87**:781-788.
7. Phillips JC, Braun R, Wang W, Gumbart J, Tajkhorshid E, Villa E, Chipot C, Skeel RD, Kalé L, Schulten K. Scalable molecular dynamics with NAMD. *J Comput Chem* 2005;**26**:1781-1802.
8. Buehler M, Keten S, Ackbarow T. Theoretical and computational hierarchical nanomechanics of protein materials: Deformation and fracture. *Progress in Materials Science* 2008;**53**:1101-1241.
9. Qin Z, Kreplak L, Buehler M. Nanomechanical properties of vimentin intermediate filament dimers. *Nanotechnology* 2009;**20**.
10. MacKerell AD, Bashford D, Bellott M, Dunbrack RL, Evanseck JD, Field MJ, Fischer S, Gao J, Guo H, Ha S, Joseph-McCarthy D, Kuchnir L, Kuczera K, Lau FT, Mattos C, Michnick S, Ngo T, Nguyen DT, Prodhom B, Reiher WE, Roux B, Schlenkrich M, Smith JC, Stote R, Straub J, Watanabe M, Wiórkiewicz-Kuczera J, Yin D, Karplus M. All-atom empirical potential for molecular modeling and dynamics studies of proteins. *J Phys Chem B* 1998;**102**:3586-3616.
11. Ackbarow T, Buehler M. Superelasticity, energy dissipation and strain hardening of vimentin coiled-coil intermediate filaments: atomistic and continuum studies. *Journal of Materials Science* 2007;**42**:8771-8787.
12. Zhang H, Ackbarow T, Buehler M. Muscle dystrophy single point mutation in the 2B segment of lamin A does not affect the mechanical properties at the dimer level. *Journal of Biomechanics* 2008;**41**:1295-1301.
13. Qin Z, Kreplak L, Buehler M. Hierarchical Structure Controls Nanomechanical Properties of Vimentin Intermediate Filaments. *Plos One* 2009;**4**.
14. Weisenhorn A, L,, Khorsandi M, Kasas S, Gotzsos V, Butt H, J,. Deformation and height anomaly of soft surfaces studied with an AFM. 1993:106-113.
15. Radmacher M, Fritz M, Hansma PK. Imaging soft samples with the atomic force microscope: gelatin in water and propanol. *Biophys J* 1995;**69**:264-270.
16. Ohashi T, Ishii Y, Ishikawa Y, Matsumoto T, Sato M. Experimental and numerical analyses of local mechanical properties measured by atomic force microscopy for sheared endothelial cells. *Biomed Mater Eng* 2002;**12**:319-327.
17. Kuznetsova TG, Starodubtseva MN, Yegorenkov NI, Chizhik SA, Zhdanov RI. Atomic force microscopy probing of cell elasticity. *Micron* 2007;**38**:824-833.
18. Rico F, Roca-Cusachs P, Gavara N, Farré R, Rotger M, Navajas D. Probing mechanical properties of living cells by atomic force microscopy with blunted pyramidal cantilever tips. *Phys Rev E Stat Nonlin Soft Matter Phys* 2005;**72**:021914.
19. Domke J, Radmacher M. Measuring the elastic properties of thin polymer films with the atomic force microscope. *Langmuir* 1998;**14**:3320-3325.